Synthesis and Characterization of Biodegradable Copolymers

For Tissue Engineering

Antonios Papadopoulos

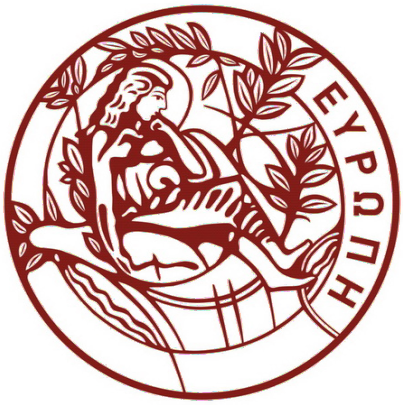

University of Crete

Undergraduate Thesis

Department of Materials Science and Technology

August 2014

Abstract

Polymers have been extensively used to fabricate scaffolds for tissue regeneration in order to repair or reconstruct damaged tissues *in vitro* or *in vivo* [1]. Chitosan (CS), polycaprolactone (PCL) and polylactide (PLA) are among the most widely studied polymers. CS, a natural polysaccharide, is a biocompatible, biodegradable and non-toxic polymer, however, it exhibits low mechanical strength and also, due to its hydrophilicity, it can be slightly dissolved in an aqueous culture medium [2]. On the other hand, PCL and PLA are biocompatible, biodegradable and nontoxic synthetic polymers, with excellent mechanical properties [3, 4]. In this work CS-*graft*-PCL (CS-*g*-PCL) and CS-*graft*-PLA (CS-*g*-PLA) copolymers were prepared by grafting hydrophobic PCL and PLA polymer chains on the CS backbone in order to alter the solubility of CS and improve its mechanical properties. First, PCL or PLA functionalized with one carboxylic acid terminal group (PCL-COOH or PLA-COOH) was prepared by ring opening polymerization of e-caprolactone or lactide, using glycolic acid as the initiator and tin octanoate as the catalyst. Polymers of different molecular weights were obtained and were characterized by gel permeation chromatography and proton nuclear resonance (^{1}H NMR) spectroscopy. Next, the PCL-COOH or PLA-COOH chains were chemically grafted onto the CS backbone via the hydroxyl groups of CS (Fig. 1) [5]. The purified products as well as the intermediates of the reaction were characterized by Attentuated Total Reflectance Fourier Transform Infrared (ATR-FTIR) and ^{1}H NMR spectroscopies. Next, thin films of the CS-*g*-PCL samples were produced using the spin coating method and cellular compatibility of the materials was examined. The 2D scaffolds were seeded with NRK cells for 7 days and the viability of the cells was tested using live-dead staining and MTT assay. The topographical characteristics of the cells attached onto the polymer surface were visualized using SEM. After a week study the cellular behavior was enhanced showing an increased cell number, very good cell attachment and proliferation.

ACKNOWLEDGEMENTS

I would like to express my special thanks to my supervisor Dr. Maria Vamvakaki, for giving me the opportunity to work in this project.

A special thanks to Maria Kaliva for the material synthesis and Georgina Kaklamani for the cell compatibility study for teaching, supervising and helping me to complete my study.

Finally I would like to express my thanks to all my colleagues Fani, Lefteris, Orestis, Thodoris, Daniel, Eua, Chara, Kostas, Panos, Dimitris, Sofia, Alexandra for helping me in everything that i needed.

Table of Contents

List of Figures

List of Tables

List of abbreviations

CS	Chitosan
PCL	Polycaprolactone
PLA	Polylactide
SDS	Sodium dodecyl sulfate
NHS	N-Hydroxysuccinimide
DCC	N,N'-Dicyclohexylcarbodiimide
THF	Tetrahydrofuran
DMF	Dimethylformamide
DMSO	Dimethyl sulfoxide
SEM	Scanning Electron Microscopy
^{1}H NMR	Proton Nuclear Magnetic Resonance
GPC	Gel Permeation Chromatography
FT-IR	Fourier Transform Infrared Spectroscopy
DMEM	Dulbecco's modified eagle's medium
MTT	3-(4, 5-Dimethylthiazol-2-yl)-2,5-diphenyltetrazolium bromide
MW	Molecular weight
DP	Degree of Polymerization
PBS	Phosphate buffered saline
UV	Ultraviolet

CHAPTER 1: Introduction

Biomaterial is any material that comes in contact with a living system. Metals, ceramics and polymers are among the most known biomaterials that have been used in medicine up to date. Metals have been widely used for load-bearing implants in orthopedics due to their high strength, high hardness, high modulus, high fatigue life, low plasticity etc. An example of a metal biomaterial is stainless steel which has been used for hip replacement [6]. On the other hand, ceramics have been used as parts of the musculoskeletal system, dental and orthopedic implants, orbital and middle ear implants, etc. An example of a ceramic biomaterial is Al_2O_3 which has been used to correct congenital deformity of vertebrae Spacers or extensors [7]. Finally, polymers represent a significant category of biomaterials because they are easy to synthesize compared to metals and ceramics, they can be manufactured in different shapes, their mechanical and physical properties can be controlled and tailored according to the use and their cost is low. Polymers have been widely used in medicine and biotechnology [8]. Some applications are in implants [9], drug delivery systems [10], dental materials [11] and materials for orthopedic and tissue engineering applications [12] as shown in Table 1.

Table 1: Polymers for biomedical applications

Polymer	Biomedical Applications
Poly(methyl methacrylate)	Intraocular lens, bone cement, dentures [13]
Poly(ethylene terephthalate)	Vascular graft [13]
Poly(dimethylsiloxane)	Breast prostheses [13]
Poly(tetrafluoroethylene)	Vascular graft, facial prostheses [13]
Polyethylene	Hip joint replacement [13] Osteochondral defects [14]
Polyurethane	Facial prostheses, blood/device interfaces [13]
Poly(lactide) poly(glycolic acid)	Bone fixation devices, scaffolds for soft and hard tissue repair, fracture fixation, articular defects, drug release and sutures.[15]
Poly(vinyl siloxane)	Dental impression materials [14]
Poly(hydroxyethyl methacrylate)	Soft contact lenses [14]

poly(caprolactone)	Bone and cartilage repair [16]

Biocompatibility is the ability of a material to interact with a living system without any advert side effect such as carcinogenesis, pyrogenicity, allergic reaction and toxic substances release. Biodegradable are the materials that can decompose by hydrolytic breakdown in the body while they are being replaced by regenerating natural tissue. The chemical by-products of the degrading materials are absorbed and released via metabolic processes of the body.

One natural polymer that has been widely used as a biomaterial is chitosan (CS). Chitosan is a biocompatible, biodegradable and non-toxic polysaccharide. CS is soluble in low pH aqueous solution and is rich in amino and hydroxyl groups (Fig.1). Non-specific reactions can be performed on the alcohol groups such as etherification and esterification reactions. By this reactions synthetic polymers can be grafted onto CS, if it's necessary, to adjust chitosan's properties for a specific application [17]. CS due to the breakable glycosidic bonds is biodegradable and is decomposed in vivo by several proteases, and mainly lysozyme. The rate of its degradation is highly related to the molecular mass of the polymer and its deacetylation degree, for example as the MW or the degree of deacetylation increases the degradation rate decreases [18]. Bhaskara Rao et al. studied Chitosan's toxicity and hemostatic potential *in vivo*. They found that chitosan is an ideal nontoxic biopolymer and it also appears that its hemostatic activity is independent of the classical cascade system [19]. Kuen Yong Lee et al. investigated the in vitro blood compatibility of CS by rheological measurements. N-hexanoyl chitosan, showed the best blood compatibility due to the increased surface hydrophobicity [20]. Chitosan's biomedical applications are limited because of its low mechanical strength compared to cytoskeleton, so it can't support cell growth e.g. for bone regeneration applications. Also due to its hydrophilicity is slightly soluble in the culture medium. A way to improve the mechanical properties and alternate the solubility of CS is to graft synthetic polymers, such as polylactide and polycaprolactone, onto the chitosan backbone [5].

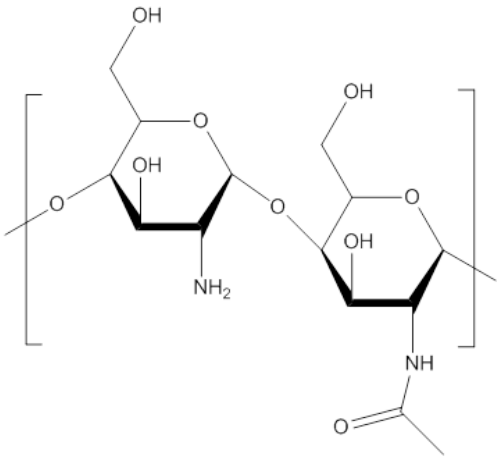

Figure 1: Chemical structure of Chitosan

Polylactide (PLA) (Fig. 2), is a biocompatible and biodegradable polymer which is widely used for biomedical and pharmaceutical applications [3]. The interest in polyesters is due to their hydrolyzable ester bonds , which render the polymer backbone biodegradable. Due to its biocompatibility PLA has been widely used in biomedical applications such as in sutures, scaffolds for tissue engineering, orthopedic devices, or drug delivery systems [21]. PLA substrates have been used for bone tissue engineering. Badami et al. investigated the effect of the substrate's topography produced by the electrospining method on osteoblasts function. Random fuse fibers with diameters ranging from 0.14 nm to 2.1 μm were produced and it was found that osteoprogenitor cells function was favored, since the cells were able to adhere and proliferate and also the density of the cells increased with increasing the fiber diameter. Moreover, the cells on fibers had a smaller projected area than cells on smooth surfaces [22]. However, PLA appears to have poor mechanical properties, such as reduced impact strength, and low thermal stability which can be a problem for certain applications.

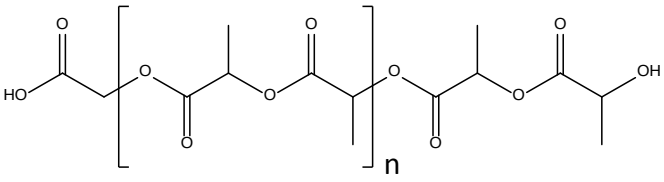

Figure 2: Chemical structure of Polylactide

Polycaprolactone (PCL) (Fig. 3), is a synthetic, semi-crystalline, linear aliphatic polyester and is biodegradable due to the susceptibility of its aliphatic ester linkages to hydrolysis. PCL has been widely used as a soft and hard-tissue compatible material including resorbable sutures, drug delivery systems and bone graft substitutes. However, applications of PCL might be limited because the degradation and resorption kinetics of PCL are considerably slower compared to other aliphatic polyesters. This is due to its hydrophobic character and high crystallinity [4]. Deborah J. et al. investigated the coating effect of two proteins, transglutaminase (tTG) and fibronectin, on PCL's biocompatibility for bone repair. PCL substrates were first coated with fibronectin and then tTG. It was found that after seeding human osteoblasts with serum free medium there was an increase on the spreading of the cells compared to the PCL surface coated with only fibronectin. The presence of tTG had no effect on human osteoblasts. Therefore, the use of tTG has potential in forming a stable tissue/biomaterial interface for application in medical devices[23]. Hutmacher et al. investigated the mechanical properties and the cellular compatibility of porous PCL scaffolds fabricated by fused deposition modeling. It was found that the mechanical properties of PCL scaffolds were ideal for tissue engineering since human fibroblasts and periosteal cells appeared to have very good behavior when seeded on these materials[24].

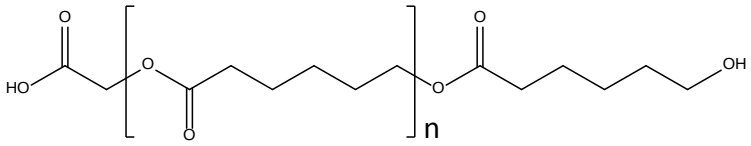

Figure 3: Chemical structure of Polycaprolactone

There have been some attempts in the literature to improve the properties of chitosan by blending it with other synthetic biocompatible polymers such as polylactide and polycaprolactone. Duarte et al. created 3D porous scaffolds from a CS-PLA blend for tissue engineering such as skin, bone and cartilage regeneration [25]. CS is hydrophilic and PLA is hydrophobic so by blending these two materials there would be phase separation. In order to prevent phase separation they used supercritical fluid technology. They claim that by using this technology they avoided phase separation and confirmed their claim by creating a 2D chemical map using IR spectroscopy which showed that chitosan and polylactide are not separated along the scaffold. In another example CS-PCL blend membranes were produced for potential biomedical applications [26]. CS

was dissolved in acetic acid and PCL was dissolved in glacial acetic acid, the two materials were mixed and homogeneous membranes were formed. Membranes from a 50% chitosan-50% PCL blend showed improved mechanical properties compared to the pure chitosan membranes and an increase of the cell number compared to the control. On the other hand, a cell compatibility study with mouse embryonic fibroblasts showed that 48 hours after seeding there was a decrease of the cell spreading area compared to the control, which limited the applicability of this material in tissue engineering applications.

Cells can interact with a material only if the material is biologically recognizable. Biologically recognizable means that certain kinds of proteins can interact and adhere on the material surface and then cells can recognize the adhesion proteins via their integrin receptors. So biological recognition increases the adhesiveness of cells which possess the integrin receptors e.g. fibroblasts integrin receptors recognize preadsorption fibronectin. After the exposure of a biomaterial in supplemented medium, the biomaterial surface recognizes proteins in less than 1 second. After a few seconds or minutes, depending on the material, a protein monolayer forms on the biomaterial surface because of continuous protein absorption. When adsorbed on a material's surface proteins change their conformation because of their relatively low structural stability, however they retain some of their activity. The protein adsorption step takes place before the cells reach the surface so the cells at first interact with the protein monolayer and not directly with the biomaterial surface. In response to the protein monolayer, cells can adhere, release active compounds, recruit other cells, grow in size and replicate. When cells finally reach and interact with the biomaterial surface they differentiate, multiply, communicate with other type of cells and reorganize themselves into tissues. Cells adjust their structure and function in order to fit in the present environment so the shape, the proliferation and the synthetic functions depend on the characteristics of the substrate. If the environment is appropriate for cells then the spreading area of cells increases and as a consequence the rate of proliferation increases [27]. It has been found that when cells are seeded on polymeric surfaces their function is favored when amine functional groups are present on the surface and cells spreading and growth are enhanced on polymeric surfaces which have hydroxyl functional groups [28].

Yuan et al. investigated the interaction of Schwann cells with CS membranes and fibers *in vitro*. It was found that Schwann cells grow on CS with spherical and long olivary shapes. Cells

encircle fibers and migrated faster on CS fibers compared to CS membranes. Moreover, cells migrate in areas that have microvilli on both fibers and membranes and also reached the minute foot to interact with the surface. Spherical cells target small surfaces, whereas, the olivary cells interact at large surfaces [29]. Venugopal et al. investigated the in vitro smooth muscle cells interaction with PCL nanofibrous matrices. It was found that on the collagen coated matrices muscle cells migrated inside them and formed smooth muscle tissue [24].

The aim of this project was to synthesize biodegradable graft copolymers, based on polylactide/polycaprolactone and CS, and test their cellular compatibility *in vitro* using NRK cells. Chitosan-*graft*-Polycaprolactone (CS-*g*-PCL) and Chitosan-*graft*-Polylactide (CS-*g*-PLA) copolymers were synthesized, characterized and fabricated in thin films for the cell compatibility study. Graft copolymers were synthesized in order to improve the mixing of the two incompatible polymeric components and avoid the macroscopic phase separation of the composite material.

CHAPTER 2: Materials and Methods

2.1 Materials

CS (MW = 110.000-150.000 gr/mol, high purity), ε-caprolactone (97 % purity, MW = 114.14gr/mol, Glycolic acid (99 % purity, MW = 76.05 gr/mol), Lactide (MW = 144.13gr/mol), SDS (≥ 98.5 % purity, MW = 288.38 gr/mol) were purchased from the Sigma-Aldrich Chemical Co. Stannous octoate (95 % purity and MW = 405.12 gr/mol) was purchased from Aldrich Chemical Co

2.1.1 Chitosan

A CS solution was prepared using the high purity polymer which was dissolved in acidified nanopure water (2% v/v CH_3COOH) at a concentration of 1% w/v.

2.1.2 Synthesis of PCL

PCL functionalized with a carboxylic acid end group was synthesized using bulk polymerization method. Liquid ε-caprolactone was mixed with glycolic acid at a mol ratio 70:1, and liquid stannous octoate at a mol ratio 70:1 to glycolic acid. The solution was mixed using a magnetic stir bar for approximately 5 mins. Continuing, a three circle of freeze-pump-thaw procedure was followed in order to remove oxygen and the mixture was placed in an oil bath at 140 $^{\circ}$C and the polymerization was carried out for 24 hrs under continuous stirring. The mixture was left to cool down at room temperature, then, THF was added until the solid polymer was dissolved and the solution was added dropwise in a ten-fold excess of methanol in order to precipitate the pure polymer (the monomer remained soluble in methanol). The methanol with monomer were decanted and the precipitated polymer was left in an oven to dry under vacuum until constant mass.

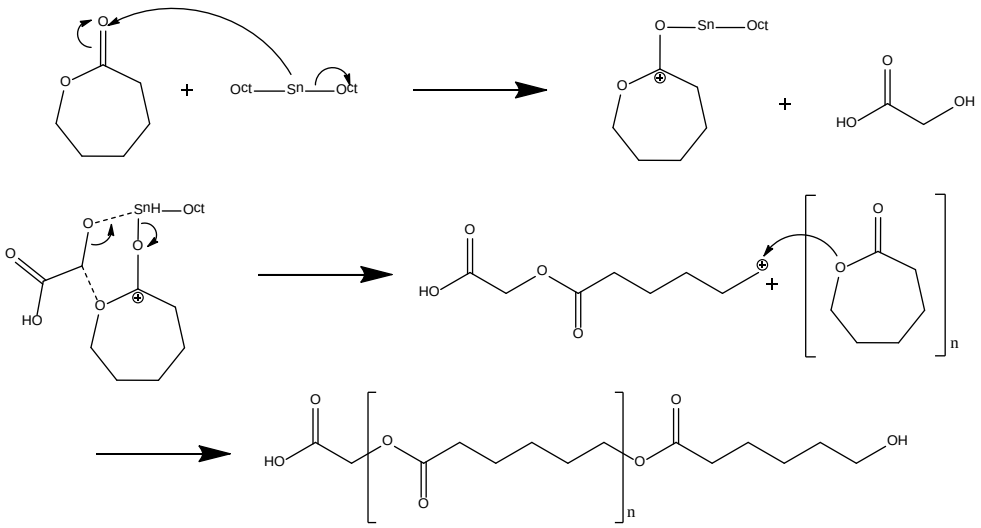

Figure 4: Mechanism of PCL ring opening polymerization [30]

2.1.3 Synthesis of PLA

PLA functionalized with a carboxylic acid end group was synthesized using the solution polymerization method. Lactide powder was mixed with glycolic acid at a mol ratio 55.5:1, liquid stannous octoate at a mol ratio 1:50 to the lactide and toluene as the reaction solvent. The concentration of lactide was 15% w/v in toluene. The solution was mixed using a magnetic stir bar for approximately 5 minutes. Next, a three circle of freeze-pump-thaw procedure was followed in order to remove oxygen and the mixture was placed in an oil bath at 110 $^{\circ}$C and the polymerization was carried out for 24 hours under continuous stirring. The mixture was left to cool down at room temperature, and then, THF was added until the solid polymer was dissolved and the solution was added dropwise in a ten fold excess of methanol in order to precipitate the pure polymer (the monomer remained soluble in methanol). Methanol and the monomer were decanted and the precipitated polymer was left in an oven to dry under vacuum until constant mass.

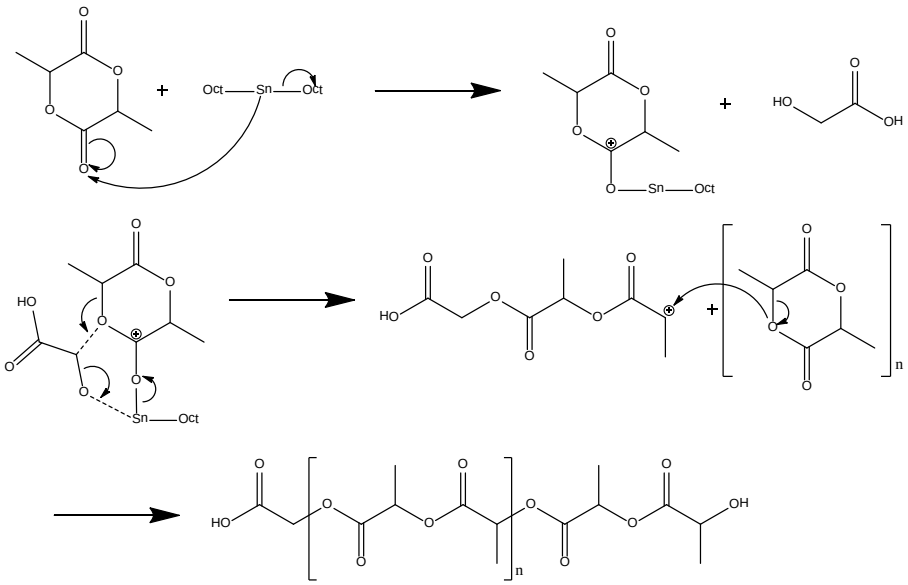

Figure 5: Mechanism of PLA ring opening polymerization [3]

2.2 Methods

2.2.1 PCL and PLA grafting onto Chitosan

In order to produce the CS-*g*-PCL and CS-*g*-PLA graft copolymers, first the hydrophilic CS had to be converted to hydrophobic so that it can be mixed with the hydrophobic PCL or PLA. For this, a 5% w/v SDS solution was prepared in nanopure water. Then the SDS solution was added in a CS solution (§ 2.1.1) and was stirred continuously for 24 hours at room temperature. The CS:SDS mol ratio was 1:2.5. The product was recovered by centrifugation at 10,000 rpm for 12 minutes and was filtered and washed repeatedly with nanopure water to remove the excess of SDS. Finally, CS-SDS was freeze dried for 24 hours.

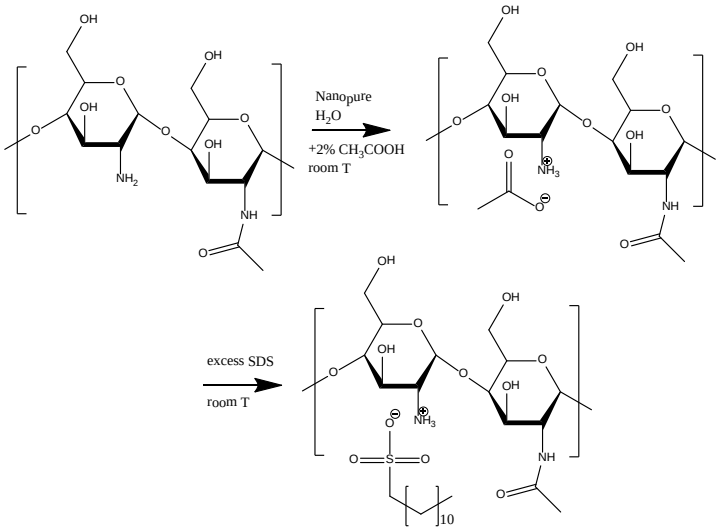

Figure 6: Hydrophobically modified CS with sodium dodecyl sulfate (SDS)

Next, the carboxylic end group of PCL or PLA had to be activated in order to graft the synthetic polymers onto chitosan. For the activation of PCL and PLA the procedure followed is described below. The polymer was first dissolved in DMF at a concentration 0.6% w/v. Next NHS and DCC were added in the solution at a mole ratio 2:1 with respect to the polymer. The solution was stirred using a magnetic stirrer for 24 hours at room temperature under nitrogen. The final product was recovered by distillation to remove DMF and then it was left in the oven to dry under vacuum until constant mass.

To produce the CS-*g*-PCL and CS-*g*-PLA graft copolymers, CS-SDS at a concentration of 0.75% w/v was dissolved in DMSO and the activated polymer (PCL or PLA) was dissolved in N-methylpyrrolidinone (3% w/v). The mass of the polymer with respect to CS-SDS was 30% w/w. The PCL or PLA solution was then mixed with the CS-SDS solution under continuous stirring and under a nitrogen atmosphere at room temperature for 48hrs. Next the solution was dialyzed against DMSO (membrane MWCO 12,000) to remove any unreacted PCL or PLA and the excess of NHS and DCC. Finally the solution was added into a 15% w/v Tris(hydroxymethyl)aminomethane aqueous solution in order to remove the SDS. The precipitate was isolated using centrifugation, washed several times with 15% w/v Tris(hydroxymethyl)aminomethane aqueous solution, DMF and nanopure water. The dry polymer was obtained by freeze drying.

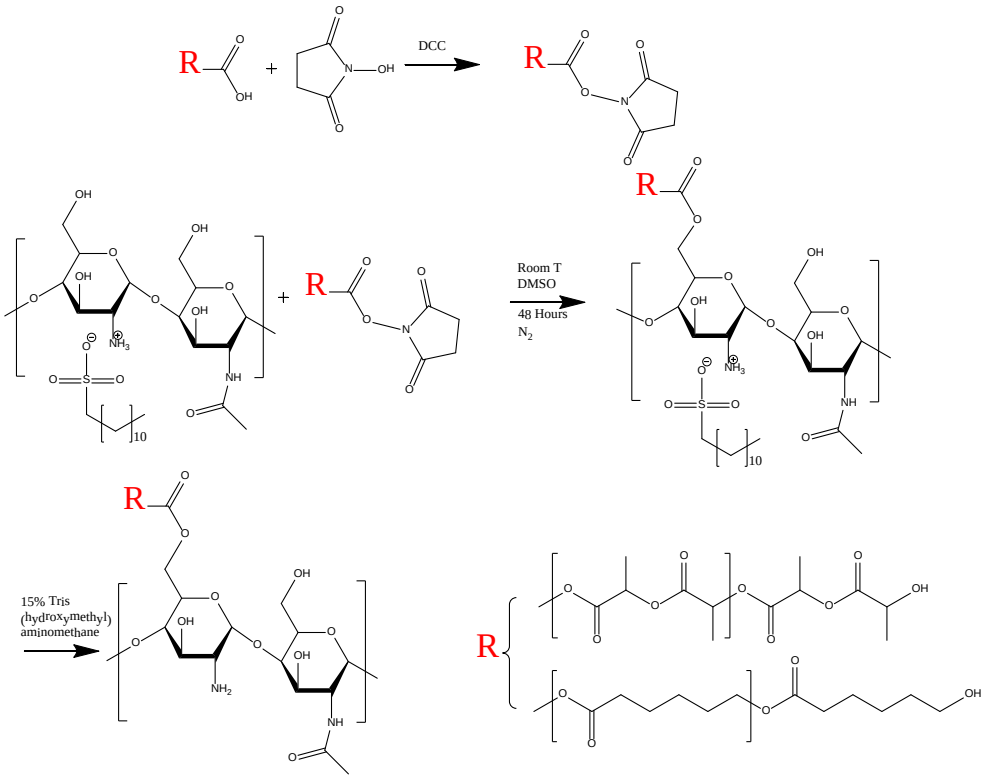

Figure 7: Activation of PCL(PLA) and grafting reaction

2.2.2 Gel Permeation Chromatography (GPC)

GPC is a type of liquid chromatography that separates analytes on the basis of their size. GPC is used to determine the molecular weight of polymers and its operation is based on porous material columns. A pump pushes the solvent thought the instrument and an injection port is used to introduce the test sample, which is first dissolved in the same solvent, into the column. As the solution flows through the column, small size molecules can enter the pore of the material, as shown in figure 8, and spend more time in the column conversely large size molecules blockade from the porous and spend less time in the column. The pore size of the columns must be similar to the polymer size. In this study, THF was used as the eluent solvent at a flow rate of 1 ml/s, the polymer concentration in THF was 4% w/v and narrow PMMA standards were used for calibration.

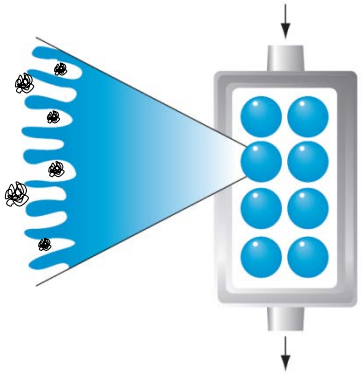

Figure 8: GPC representation

2.2.3 Nuclear Magnetic Resonance (^{1}H NMR) Spectroscopy

^{1}H NMR spectroscopy is used in order to identify the chemical composition of a material and to monitor the reaction progress. NMR is a physical phenomenon in which nuclei in a magnetic field absorb and re-emit electromagnetic radiation which allows the observation of specific quantum mechanical magnetic properties of the atomic nucleus. In our case we observe the absorbance and re-emission of the hydrogen nucleus. In this study ^{1}H NMR spectroscopy was used in order to verify the molecular structure and purity of the synthesized polymers PLA and PCL, of Chitosan-SDS and to determine the composition of the final copolymers CS-*g*-PCL and CS-*g*-PLA.

2.2.4 Fourier Transform Infrared Spectroscopy (FT-IR)

FT-IR spectroscopy is used in order to identify the chemical composition of a material and weather the reaction is complete. The technique is based on infrared radiation (IR), which is passed through the sample. Depending of the material, specific frequency of IR radiation is absorbed by the sample and the rest is transmitted. An infrared spectrum contains bands which represent the frequencies of vibration between the chemical bonds of the atoms present in the material. Therefore, a qualitative analysis of different types of materials can be done. In this study FTIR spectroscopy was used in order to identify the chemical structure of the final copolymers CS-*g*-PCL and CS-*g*-PLA. The measurements were performed in the frequency range between 400 and 4000 cm^{-1} and 30 scans were taken for each spectrum. A background scan was taken prior to each measurement and was subtracted from the sample spectra.

2.2.5 Thin Film Preparation

2D thin films on glass substrates were prepared in order to use them for cell culture. Before the film preparation, the glass substrates 1cm x 1cm were purified from organic substances using Helmanex to make the surface more hydrophilic and thus prepare a more homogenous thin film on the surface. After the purification step, the substrates were washed with water, ethanol and finally dried with a nitrogen flow. The spin coating technique was used in order to prepare 2D

thin films. 140 µl of a 0.5 % w/v CS-*g*-PCL solution was used in a 1:1 acetic acid:water mixture. The parameters used in the spin coating technique were RPM = 2000, time = 180 s and acceleration = 2000 RPM/s. After the film formation the materials was left in an oven under vacuum at 50 °C overnight and were then neutralized by dipping in a 1M NaOH solution.

2.3 Cell Culture Experiments

All chemicals for the cell culture experiments were obtained from Thermo-Scientific, FR. In this study, cell compatibility tests were performed using NRK (Normal Rat Kidney) Epithelial Cells. The cell culture was prepared and afterwards the cells were seeded on the polymeric substrates. NRK were cultured in T175 tissue culture flasks (Corning, NY, USA) in supplemented cell culture medium (S-DMEM with 10% (v/v) SVF, 1% (v/v) L-Glutamine and 1% (v/v) Penicillin/Streptomycin) in incubator (Thermo Scientific, Fr) at 37°C, CO_2 at 5% and 100% relative humidity. Cell were fed every 3rd day of culture and trypsinised on day 7 after having reached ~ 70% confluency. The 2D thin polymer films prepared by spin coating were sterilized by UV light and ethanol before cell seeding. Day 1, 3 and 7 were tested using the following techniques: SEM, live-dead staining, Hoechst staining, optical microscopy and MTT assay for two population of cells 10,000 cells/sample and 50,000 cells/sample. Live-dead staining was used in order to observe the cellular viability, Hoechst staining was used to stain the DNA of the attached cells, SEM was employed in order to evaluate the cells topographical characteristics and MTT assay was used to determine the approximate cell number over a period of 7 days.

2.3.1 Fluorescence Microscopy

Fluorescence Microscopy is based on a mirror which reflects only a specific wavelength. The mirror is placed in an angle of 45^o compared to the UV light beam so that the UV light can pass through the mirror, absorbed from the stain in the sample and then re-emit at higher wavelength which can reflect from the mirror to the observer. Fluorescence microscopy is used to assess cell viability using PI (propidium iodide), AM (calcein acetoxymethyl ester) and Hoechst staining. For PI staining a mirror that reflects only at 617 nm wavelength is used, for AM staining a mirror

that reflects only at 520 nm wavelength is used and for Hoechst staining a mirror that reflects only at 461 nm wavelength is used.

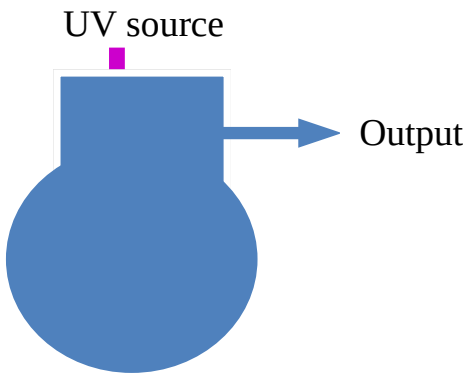

Figure 9: Fluorescence Microscopy Representation

2.3.2 Scanning Electron Microscopy

SEM (Hitachi 4800) was used to visualize the cell seeded surfaces. The operating voltage was 5 kV and the working distance was 10 mm. Prior to testing, the cell seeded samples were chemically fixed using 5% v/v glutaraldehyde for 48 h at 0°C and then dehydrated with 30, 50, 70, 90% v/v aqueous ethanol solutions for 30 mins followed by 100% dried ethanol for additional 30 mins. Finally, the specimens were coated with Au by a sputtering method to obtain a final film thickness of 10 nm

2.3.3 MTT Assay

In order to quantify the approximate number of viable cells on the surface of the seeded polymeric samples, a tretrazolium assay as used on days 1, 3, and 7. 100 μL yellow MTT (5μgr/ml) (3-(4,5-Dimethylthiazol-2-yl)-2,5-diphenyltetrazolium bromide) solution was added to each sample and incubated at 37°C at 5% CO2 and 100% relative humidity for 4 h to allow the tetrazolium ring in the salt to cleave to mitochondrial dehydrogenases and form purple formazan crystals. After incubation, these crystals were dissolved in 2 mL of 4% v/v hydrochloric acid in isopropanol. The absorbance of the dissolved crystal solution was measured at 620 nm (Cecil, Cambridge, UK) and compared to a standard curve to give an approximate cell number.

CHAPTER 3: Results and Discussion

3.1 PCL Characterization

GPC and ^{1}H NMR spectroscopy were used in order to determine the molecular weight of the synthesized polymer. For GPC analysis we used PMMA standards for calibration, 2 w/v % PCL in THF and THF as the eluent. Figure 10 shows the GPC graph of the synthesized PCL sample.

Figure 10: Gel permeation chromatogram of PCL.

Table 2: Molecular characteristics of the synthesized PCL.

M_n (gr/mol)	M_w (gr/mol)	$\frac{M_w}{M_n}$
8,100	10,300	1.26

The molecular weight and the polydispersity of PCL were calculated and are presented in Table 2. Moreover, in the GPC chromatogram of PCL the absence of extra peaks at higher elution times indicates that the final product is pure without any traces of oligomers or unreacted monomers.

Figure 11 shows the ^{1}H NMR spectrum of the synthesized PCL sample. The ^{1}H NMR spectrum of PCL was obtained by dissolving 1.5% w/v PCL in $CDCl_3$.

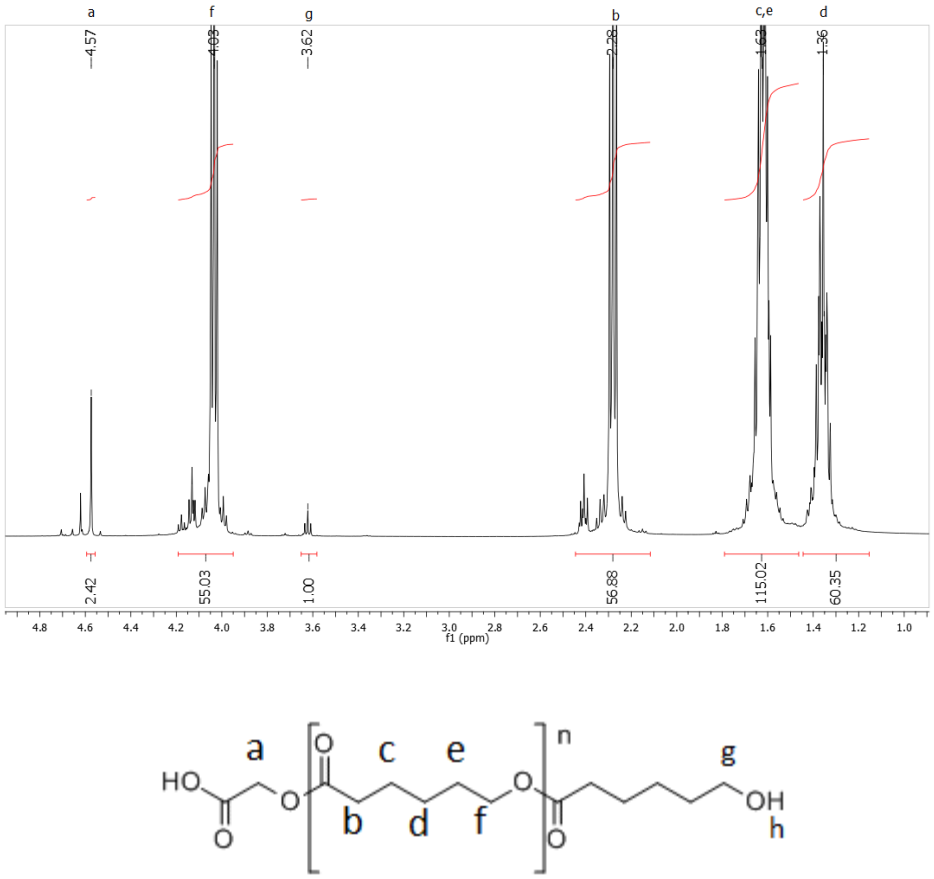

Figure 11: ^{1}H NMR spectrum of PCL.

Peak a corresponds to the methylene protons located next to the carboxylic end group of the polymer chain while the characteristic peaks b, c, d, e and f correspond to the repeat units of the polymer chain [4]. The molecular weight of the polymer and the degree of polymerization (DP) were determined by comparing the integrals for peaks g and d corresponding to methylene protons next to hydroxyl end group and to methylene protons from the repeat units respectively.

$$DP = 60$$

$$M_n = 6{,}848 \frac{gr}{mol}$$

There is a significant difference in the calculated molecular weights by the ^{1}H NMR and GPC techniques. The most accurate molecular weight is that obtained by ^{1}H NMR because the calibration in GPC was carried out with PMMA standards.

3.2 PLA Characterization

GPC and ^{1}H NMR spectroscopy were used in order to determine the molecular weight of the synthesized polymer. For GPC analysis we used PMMA standards for calibration, 2 w/v % PLA in THF and THF as the eluent. Figure 12 shows the GPC graph of the synthesized PLA sample.

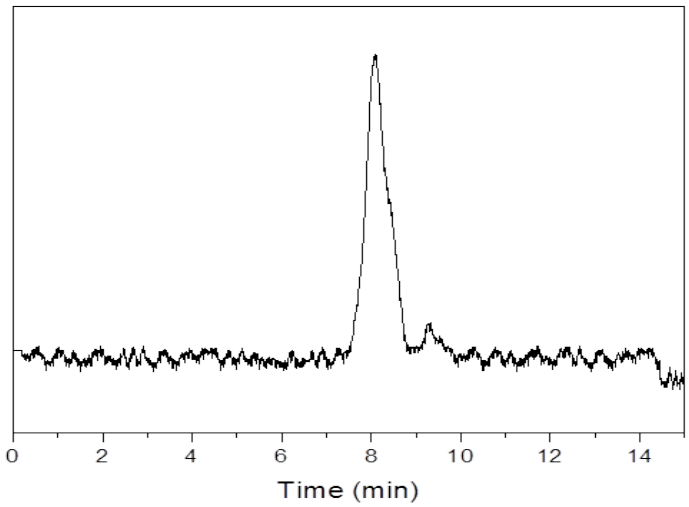

Figure 12: Gel permeation chromatogram of PLA.

Table 3: Molecular characteristics of the synthesized PLA

M_n (gr/mol)	M_w (gr/mol)	$\frac{M_w}{M_n}$
6,400	8,150	1.27

The molecular weight and the polydispersity of the synthesized PLA were calculated and are presented in Table 3. The small peak between 9 and 10 minutes of elution time may correspond to a small amount of PLA oligomer left in the product.

Figure 13 shows the ^{1}H NMR spectrum of the synthesized PLA. The ^{1}H NMR spectrum of PLA was obtained by dissolving 1.5% w/v PLA in $CDCl_3$

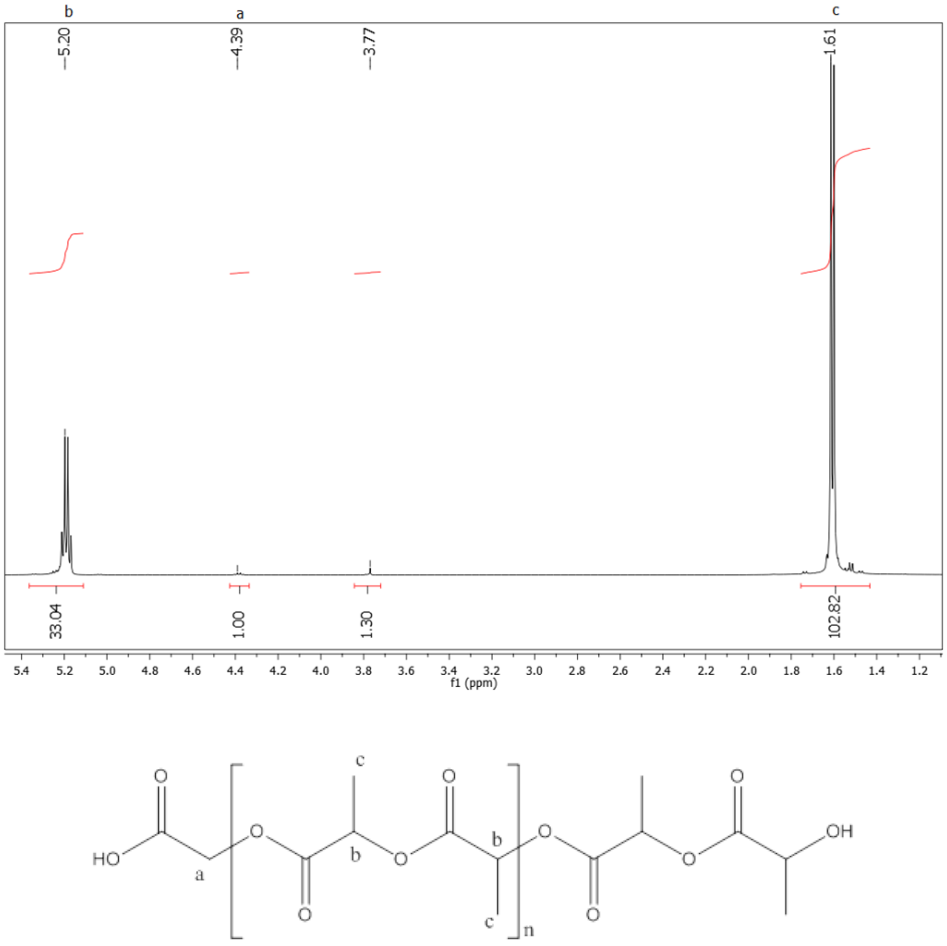

Figure 13: ^{1}H NMR spectrum of PLA.

Peak a corresponds to the methylene protons next to the carboxylic end group and the characteristic peaks b and c correspond to the repeat units of the polymer chain [31]. The molecular weight of the polymer and the degree of polymerization were determined by comparing the integrals for the peaks a and b corresponding to methylene protons next to carboxylic end group and to methylene protons from the repeat units respectively.

$$DP = 33$$

$$M_n = 4{,}756 \frac{gr}{mol}$$

3.3 CS-SDS Characterization

^{1}H NMR spectroscopy was used to verify the binding of SDS onto CS to render the latter hydrophobic, Figure 14 shows the ^{1}H NMR spectrum of the modified CS with SDS (CS-SDS) in d_6-DMSO.

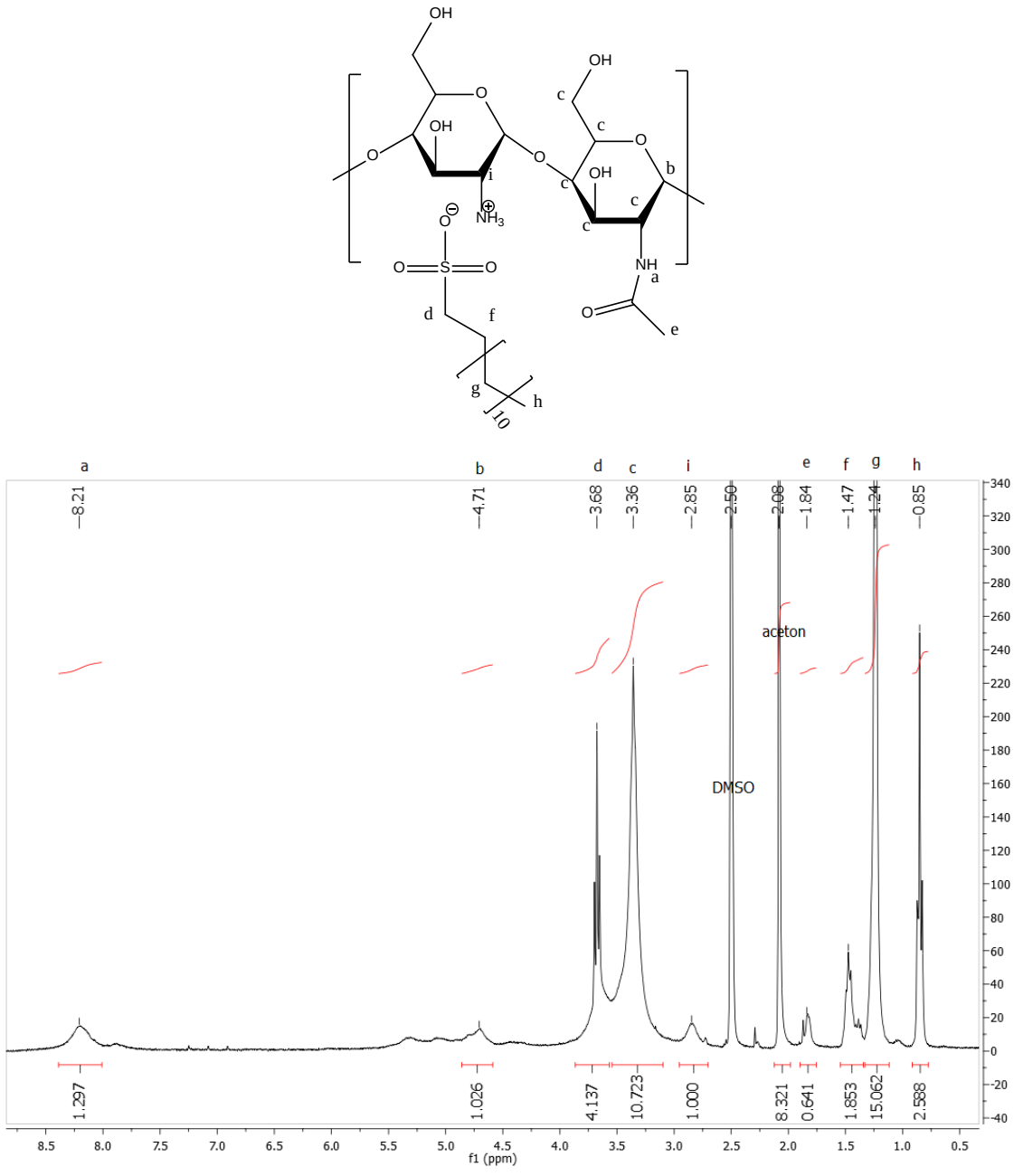

Figure 14: Chemical structure and ^{1}H NMR spectrum of CS-SDS

The degree of acetylation of CS was determined by rationing the integrals of peaks i and e and was found DA = 18 %. The presence of SDS was confirmed by the characteristic peaks h, g, f and d in the ^{1}H NMR spectrum which correspond to the methylene groups of the aliphatic tail of SDS. The CS peaks are peak i which corresponds to the hydrogen atoms next to the positively charged amino group and e which is due to the three hydrogen atoms of the acetyl group of CS [32].

3.4 CS-*g*-PCL Characterization

After the grafting reaction the ^{1}H NMR spectrum of the product was taken in order to confirm the successful synthesis of the graft copolymer and to determine the copolymer composition and the grafting density of PCL onto CS. The ^{1}H NMR spectrum of CS-*g*-PCL was obtained by dissolving 1% w/v CS-*g*-PCL in D_2O:deuturated TFA at a ratio of 1:1. Figure 15 shows the ^{1}H NMR spectrum of the final copolymer CS-*g*-PCL.

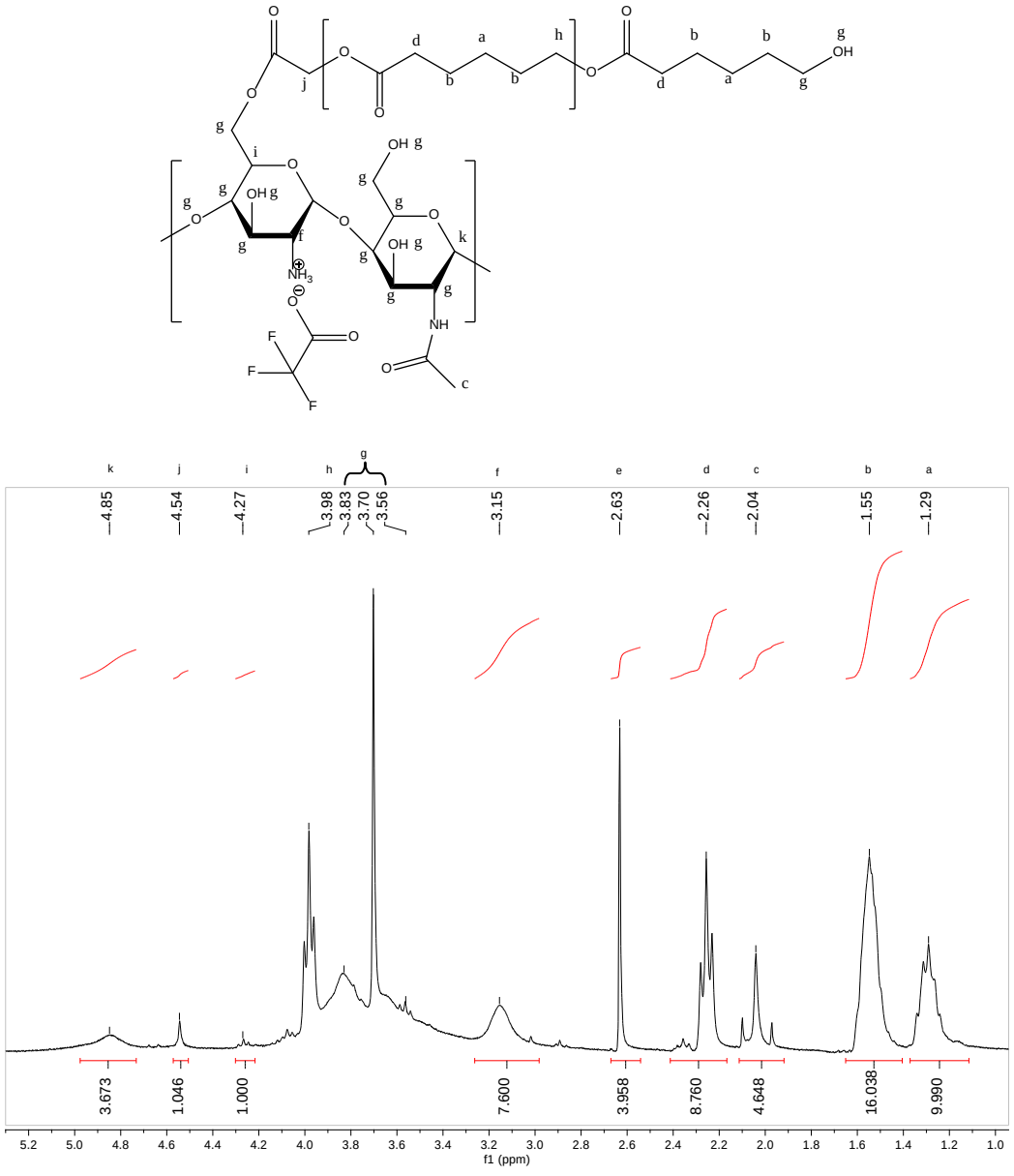

Figure 15: Chemical structure and ^{1}H NMR spectrum of CS-*g*-PCL

The characteristic peaks a, b, d, h correspond to PCL and the peaks of CS are i and e as assigned above. The peaks at 3.70 and 2.63 ppm correspond to the solvent. The grafting density was determined by rationing the integrals of peaks b and f for the given degree of deacetylation. The mole ratio of CL to the monomer units of CS was found 1:134 which results in a grafting density of 1 PCL chain for every 134 CS monomer units and a copolymer composition of 31% w/w PCL.

Figure 16 shows the FT-IR spectra of CS, PCL and CS-*g*-PCL. FTIR was used to verify qualitatively the successful synthesis of the final CS-*g*-PCL copolymer.

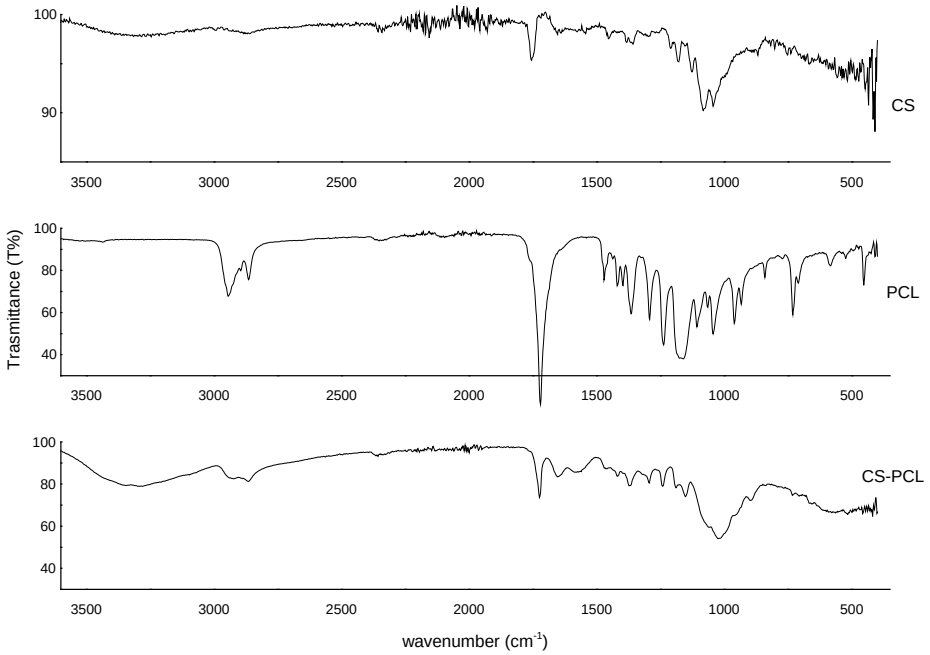

Figure 16: FTIR spectra of CS, PCL, and CS-*g*-PCL.

Table 4: FTIR wavenumbers for CS-*g*-PCL

Wavenumber (cm^{-1})	Bond Vibration
1240-1150	- C–O
1730	- C=O
2950-2830	$-CH_2$, -CH
1150-950	C–O, pyranose
3600-3100	-OH,-NH
1600–1585	C–C stretch (in ring)

The characteristic peak of chitosan is between 3600-3100 cm^{-1} which corresponds to the hydroxyl and amino group vibrations. The peak is observed in both the CS and CS-*g*-PCL spectra, see Figure 16, and indicate the presence of CS in the final product. The characteristic peak for PCL is found between 2950-2830 cm^{-1} which corresponds to the CH_2 vibrations and is observed in both the PCL and the CS-*g*-PCL spectra.

3.5 CS-*g*-PLA Characterization

After the grafting reaction the ^1H NMR spectrum of the product was recorded in order to confirm the successful synthesis of the graft copolymer and to determine the grafting density of PLA to CS and the copolymer composition. The ^1H NMR spectrum of CS-*g*-PLA was obtained by dissolving 1% w/v CS-*g*-PLA in D_2O: deuturated TFA at a ratio of 1:1. Figure 15 shows the ^1H NMR spectrum of the final copolymer CS-*g*-PCL.

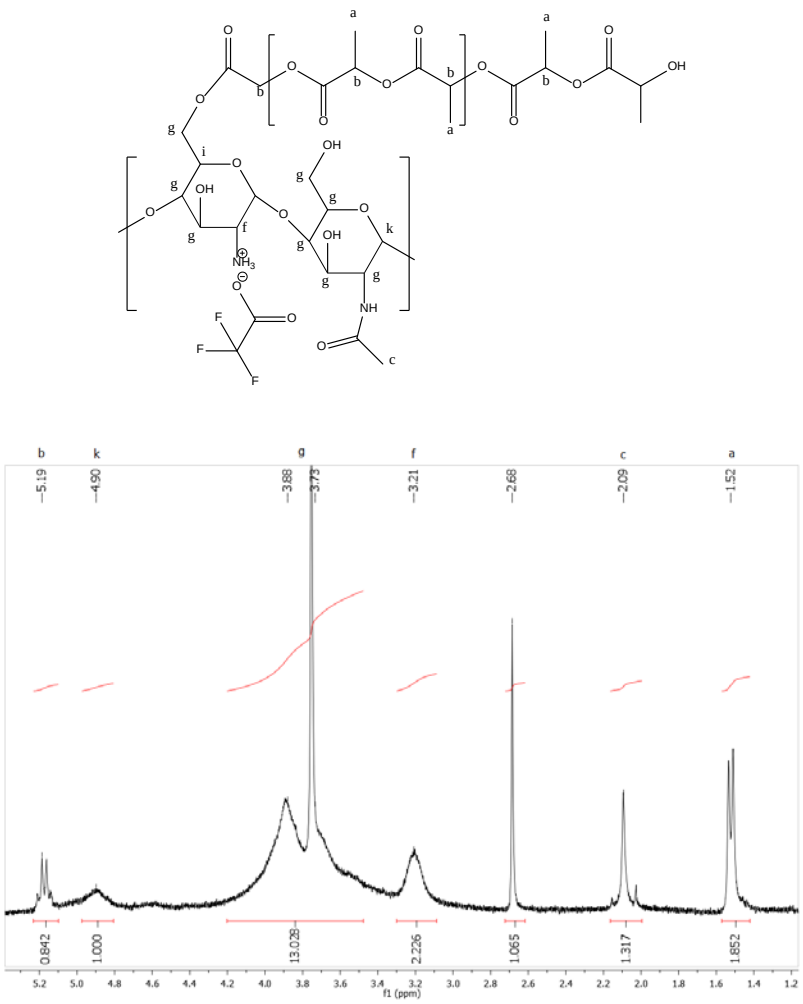

Figure 17: Chemical structure and ^{1}H NMR spectrum of CS-*g*-PLA

The characteristic peaks a and b correspond to PLA and the peaks of CS are i attributed to the hydrogen atoms next to the positively charge amino group and e due to the three hydrogen atoms in the acetyl group of CS. The peaks of CS were shifted compared to those reported by Yan Wu et al. because the graft copolymer was dissolve in $(CD_3)_2SO$ instead of D_2O and deuturated TFA [33]. The grafting density was determined by rationing the integrals of peaks b and f for the given degree of deacetylation. The mole ratio of LA to the monomer units of CS was found 1:268 which results in a grafting density of 1 PLA chain for every 268 CS monomer units and a copolymer composition of 10% w/w PCL.

To verify the final CS-*g*-PLA copolymer structure, FTIR spectra were recorded before and after the grafting procedure. Figure 18 shows the FTIR spectra of CS, PLA and CS-*g*-PLA.

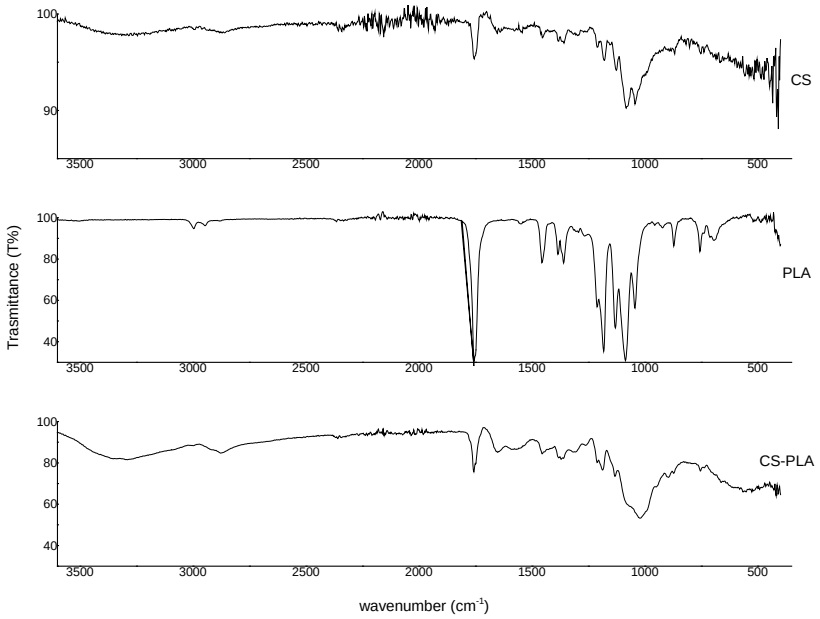

Figure 18: FTIR spectra of CS, PLA, and CS-*g*-PLA.

Table 5: FTIR wavenumbers for CS-*g*-PLA

Wavenumber (cm^{-1})	Bond Vibration
1240-1150	- C–O
1730	- C=O
2950-2830	$-CH_3$, -CH
1150-950	C–O, pyranose
3600-3100	-OH,-NH
1600–1585	C–C stretch (in ring)

The characteristic peak of chitosan is between 3600-3100 cm^{-1} which corresponds to the hydroxyl and amino group vibrations. The peak is observed in both the CS and CS-*g*-PLA spectra, see Figure 18, and indicate the presence of CS in the final product. The characteristic

peak for PLA is found between 2950-2830 cm^{-1}which corresponds to the CH_2 vibrations and is observed in both the PLA spectra and the CS-*g*-PLA spectra.

3.6 Cell Compatibility Studies

Live-dead staining was conducted in order to investigate the NRK cell viability. Figure 19 shows the live-dead staining for day 1, 3 and 7 for the CS-*g*-PCL material surface seeded with 10,000 cells/sample at day 0. Figure 20 shows the live-dead staining for day 1, 3 and 7 for the CS-*g*-PCL material surface seeded with 50,000 cells/sample at day 0.

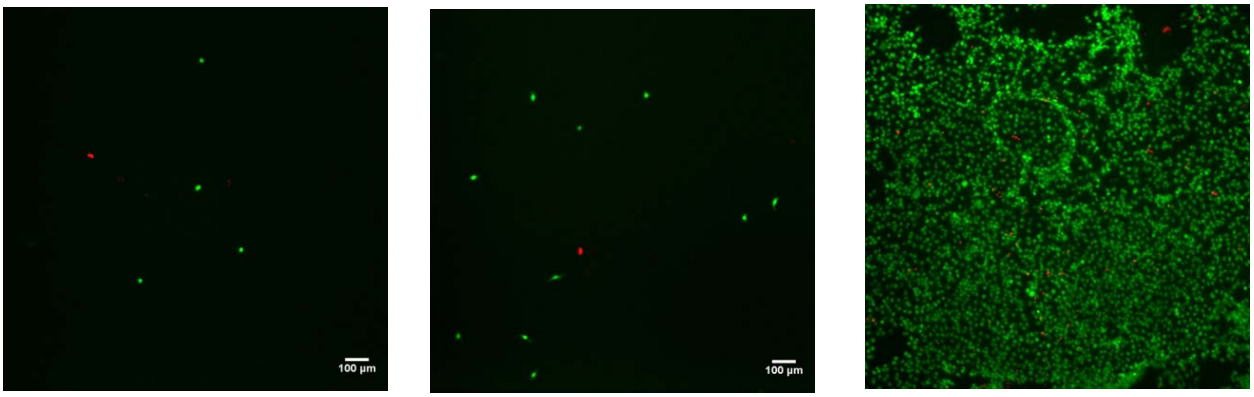

Figure 19: PI/AM staining for Day 1, 3 and 7 respectively, seeded with 10,000 cells/sample

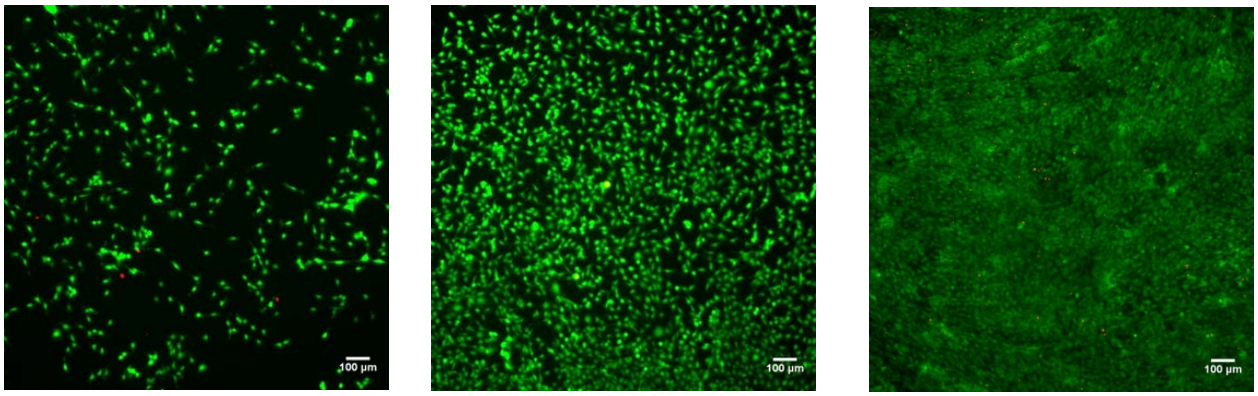

Figure 20: PI/AM staining for Day 1, 3 and 7 respectively, seeded with 50,000 cells/sample

In figures 19 and 20 the cell viability with PI/AM staining is shown, where the green color represents the live cells (AM staining) and the red represents the dead cells (PI staining). For

both populations cells attach well and proliferate from day 1 to day 7. For the 50,000 cells/sample population at day 7 the sample has almost reached its maximum confluent.

Next, Hoechst staining was used to stain the DNA of the attach cells on the CS-*g*-PCL material surface. Figure 21 shows the Hoechst staining for day 1,3 and 7 of NRK cells seeded with 10,000 cells/sample at day 0. Figure 22 shows the Hoechst staining for day 1, 3 and 7 of NRK cells seeded with 50,000 cells/sample at day 0.

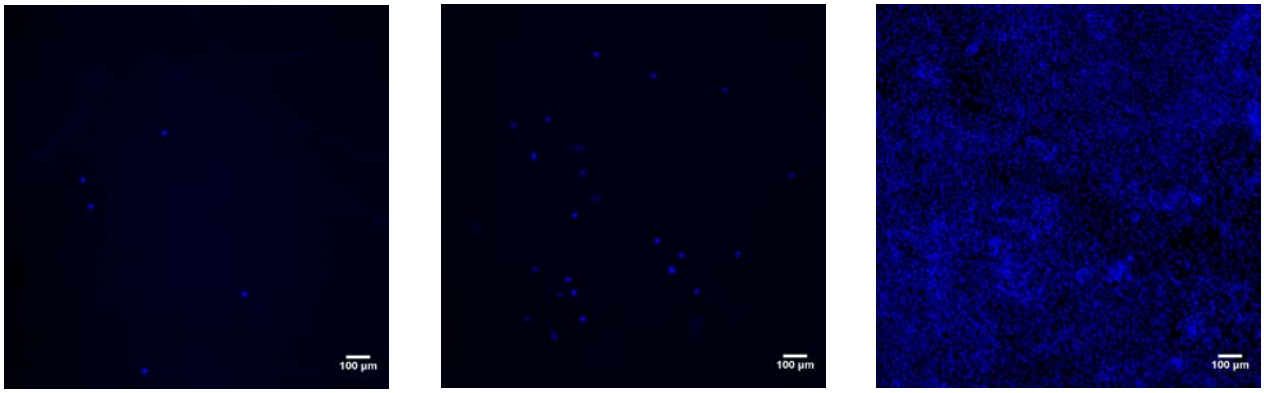

Figure 21: Hoechst staining for Day 1, 3 and 7 respectively, seeded with 10,000 cells/sample

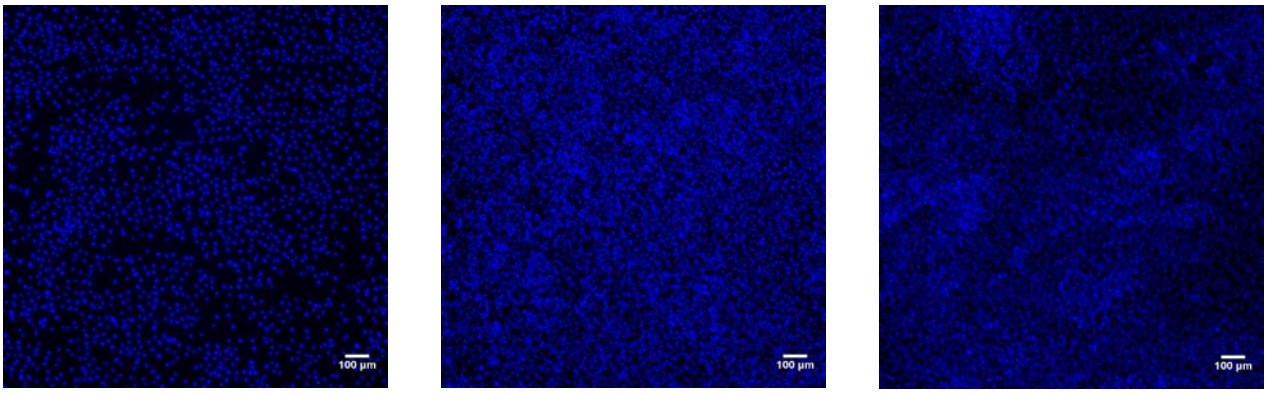

Figure 22: Hoechst staining for Day 1, 3 and 7 respectively, seeded with 50,000 cells/sample

In figures 21 and 22 the cell viability with Hoechst staining is shown, where the blue color represents the live cells core. For both populations cells attach and proliferate from day 1 to day 7.

Figures 23, 24 and 25 show the SEM images for Day 1, 3 and 7 respectively for the NRK cell culture seeded with 10,000 cells/sample at day 0 onto the CS-*g*-PCL material.

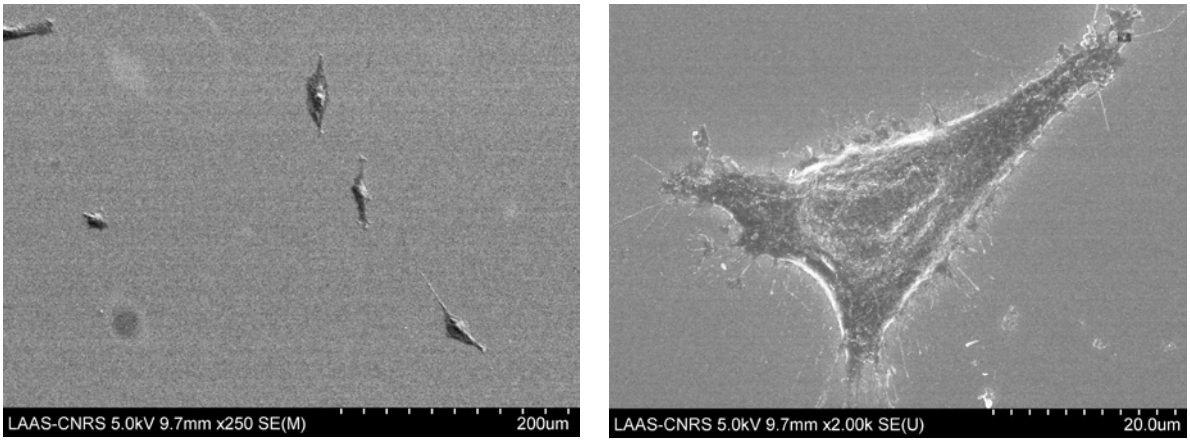

Figure 23: SEM images for Day 1 seeded with 10000 cells/sample

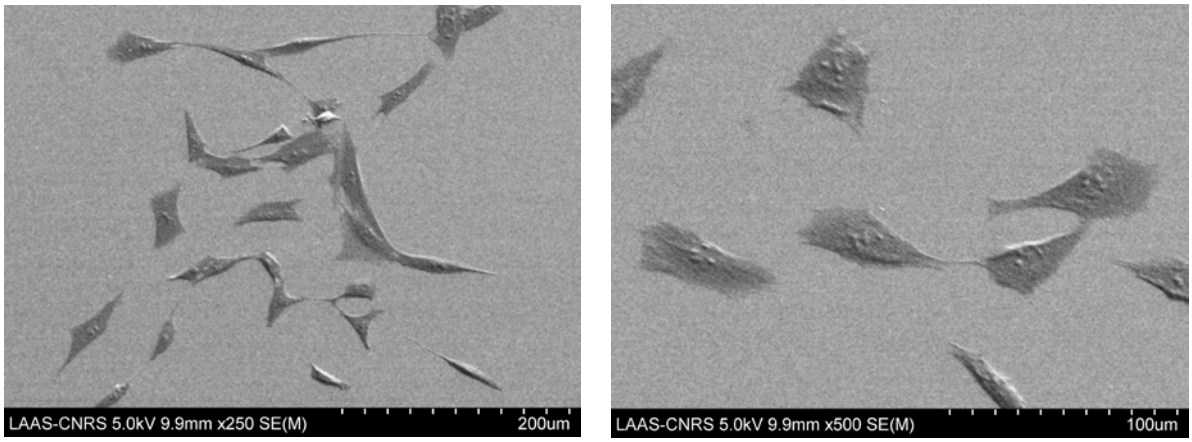

Figure 24: SEM images for Day 3 seeded with 10000 cells/sample

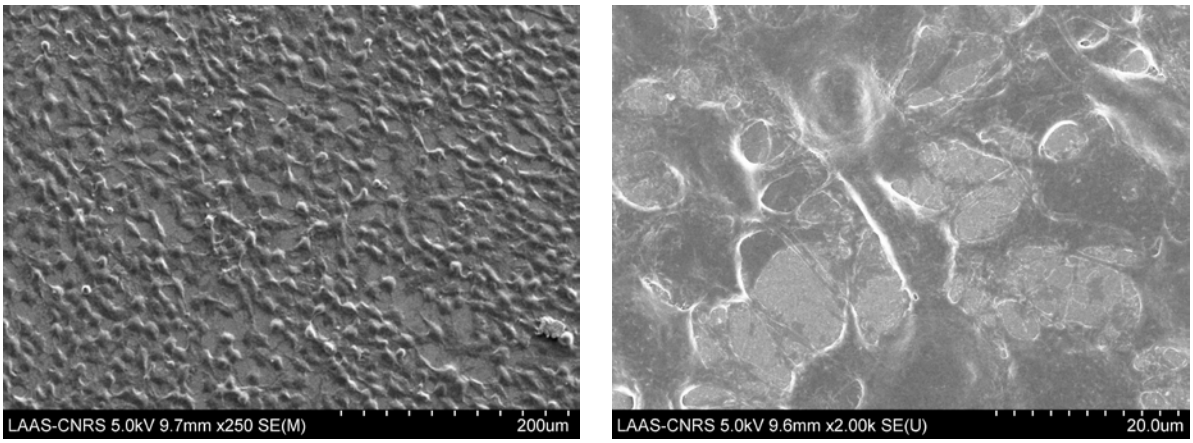

Figure 25: SEM images for Day 7 seeded with 10000 cells/sample

Figures 26 and 27 show the SEM images for Day 1 and 7 respectively for the NRK cell culture seeded with 50,000 cells/sample at day 0 onto the CS-*g*-PCL material.

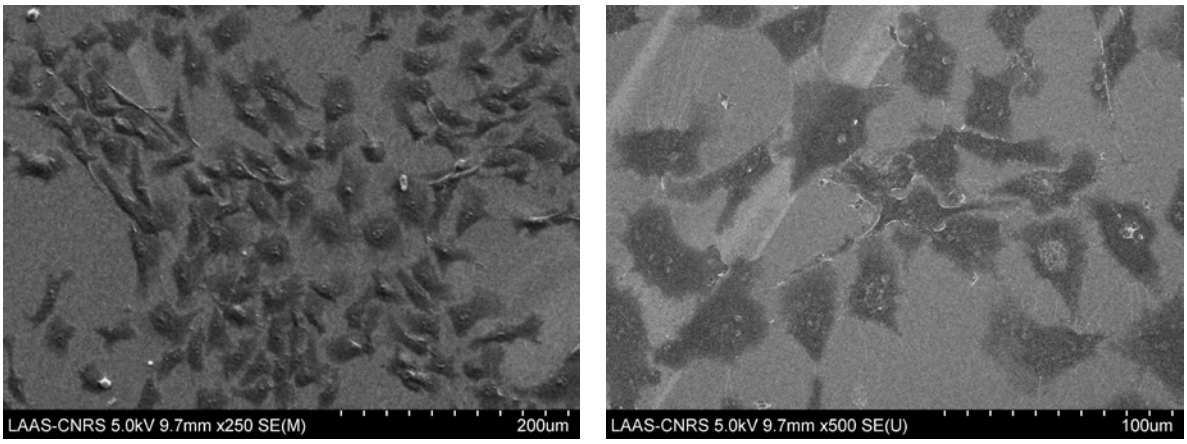

Figure 26: SEM images for Day 1 seeded with 50000 cells/sample

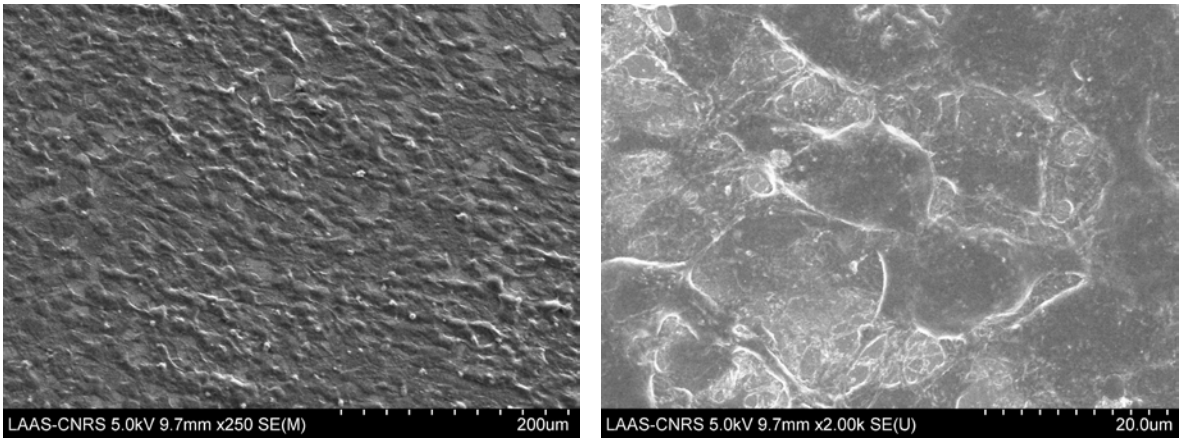

Figure 27: SEM images for Day 7 seeded with 50000 cells/sample

The NRK cells attach on the surface using cytoplasmic projections as seen in Figure 23.For both populations the NRK cells attach and proliferate from day 1 to day 7 and neighbor cells communicate with each other using intercellular junction as seed in Figure 25 and 27 in order to organize into tissue.

Figure 28 shows the MTT Assay which integrates the approximate cell number for Day 1, 3 and 5 for CS-*g*-PCL seeded with 10,000 and 50,000 cells/sample.

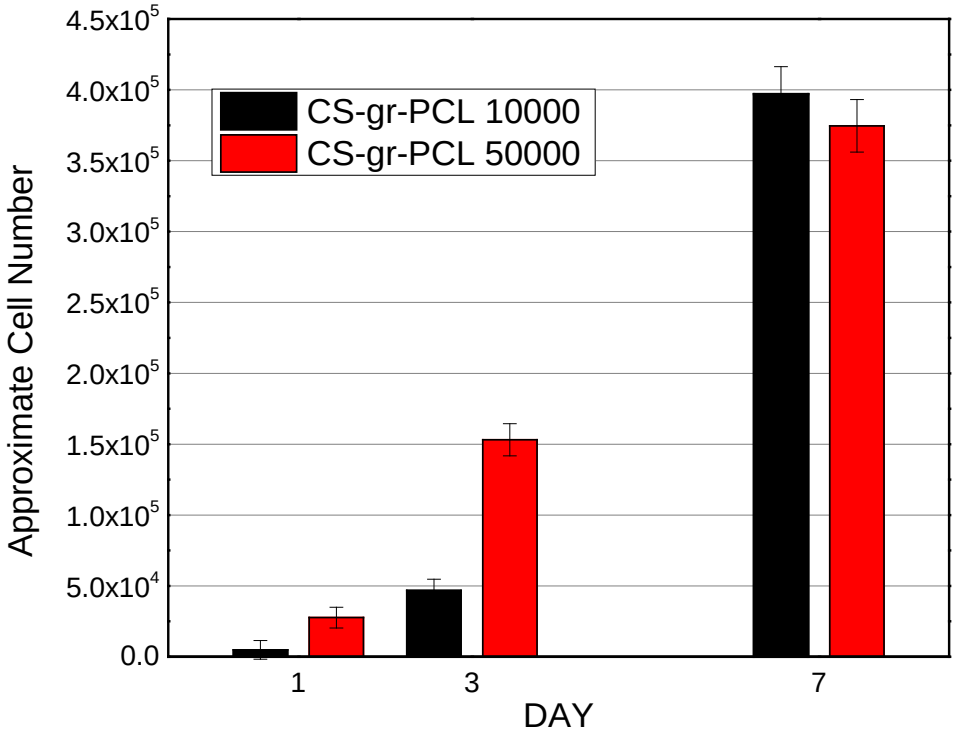

Figure 28: MTT assay on CS-*g*-PCL for Day 1, 3, 7 seeded with 10000 and 50000 cells/sample

From the MTT assay we observe that for both populations the approximate cell number rises by about 1 order of magnitude. On day seven the approximate cell number on CS-*g*-PCL seeded with 10000 cells/sample is greater than the approximate cell number seeded with 50000 cells/sample because in the second sample on day seven the cells were very confluent resulting in a significant amount of cells peeling off from the substrate in the form of tissue.

CHAPTER 4: Conclusions

In this project graft copolymers of CS-*g*-PLA and CS-*g*-PCL were successfully synthesized. First, PCL and PLA functionalized with carboxylic terminal groups were successfully synthesized and the molecular weights calculated by ^{1}H NMR were found to be 6848 gr/mol for PCL and 4756 gr/mol for PLA.. After the grafting reaction ^{1}H NMR and FTIR spectroscopy were used and both confirmed the chemical structure of the final copolymers and allowed to calculate the grafting density by ^{1}H NMR which was found to be one PCL chain for every 134 CS monomer repeat units for the CS-*g*-PCL copolymer and one PLA chain for every 268 CS monomer repeat units for the CS-*g*-PLA copolymer. A cell compatibility study was conducted for CS-*g*-PCL which showed that over seven days of cell culture cells attach well and proliferated on the surface of the thin films. Therefore, we conclude that CS-*g*-PCL shows good *in vitro* biocompatibility.

Future work includes further characterization of the 2D thin films on glass substrates (film thickness and roughness) in order to assess their influence on the cell behavior. A cell compatibility study for the CS-*g*-PLA graft copolymer will be also conducted. Finally, for both copolymers, CS-*g*-PLA and CS-*g*-PCL, an extended cell compatibility study for longer time than 7 days and for different cell types will be carried out.

List of references

1. Hubbell, J. A. *Nat Biotech* **1995,** 13, (6), 565-576.
2. Madihally, S. V.; Matthew, H. W. T. *Biomaterials* **1999,** 20, (12), 1133-1142.
3. Schwach, G.; Coudane, J.; Engel, R.; Vert, M. *Journal of Polymer Science Part A: Polymer Chemistry* **1997,** 35, (16), 3431-3440.
4. Kweon, H.; Yoo, M. K.; Park, I. K.; Kim, T. H.; Lee, H. C.; Lee, H.-S.; Oh, J.-S.; Akaike, T.; Cho, C.-S. *Biomaterials* **2003,** 24, (5), 801-808.
5. Chatzinikolaidou, M.; Kaliva, M.; Batsali, A.; Pontikoglou, C.; Vamvakaki, M. *Current Pharmaceutical Design* **2014,** 20, (12), 2030-2039.
6. Ren, L.; Yang, K. *Journal of Materials Science & Technology* **2013,** 29, (11), 1005-1010.
7. Thamaraiselvi, T. V.; Rajeswari, S. *Trends Biomater. Artif. Organs* **2004,** 18, (1), 9-17.
8. Schieker, M.; Seitz, H.; Drosse, I.; Seitz, S.; Mutschler, W. *Eur J Trauma* **2006,** 32, (2), 114-124.
9. Hutmacher, D. W. *Biomaterials* **2000,** 21, (24), 2529-2543.
10. Pasparakis, G.; Manouras, T.; Vamvakaki, M.; Argitis, P. *Nat Commun* **2014,** 5.
11. O'Brien, W. J. Dental Materials and Their Selection. University of Michigan.
12. Mikos, A. G.; Bao, Y.; Cima, L. G.; Ingber, D. E.; Vacanti, J. P.; Langer, R. *Journal of Biomedical Materials Research* **1993,** 27, (2), 183-189.
13. Nair, L.; Laurencin, C., Polymers as Biomaterials for Tissue Engineering and Controlled Drug Delivery. In *Tissue Engineering I*, Lee, K.; Kaplan, D., Eds. Springer Berlin Heidelberg: 2006; Vol. 102, pp 47-90.
14. Seal, B. L.; Otero, T. C.; Panitch, A. *Materials Science and Engineering: R: Reports* **2001,** 34, (4–5), 147-230.
15. Athanasiou, K. A.; Niederauer, G. G.; Agrawal, C. M. *Biomaterials* **1996,** 17, (2), 93-102.
16. Williams, J. M.; Adewunmi, A.; Schek, R. M.; Flanagan, C. L.; Krebsbach, P. H.; Feinberg, S. E.; Hollister, S. J.; Das, S. *Biomaterials* **2005,** 26, (23), 4817-4827.
17. Croisier, F.; Jérôme, C. *European Polymer Journal* **2013,** 49, (4), 780-792.
18. Yuan, Y.; Chesnutt, B. M.; Wright, L.; Haggard, W. O.; Bumgardner, J. D. *Journal of Biomedical Materials Research Part B: Applied Biomaterials* **2008,** 86B, (1), 245-252.
19. Rao, S. B.; Sharma, C. P. *Journal of Biomedical Materials Research* **1997,** 34, (1), 21-28.
20. Lee, K. Y.; Ha, W. S.; Park, W. H. *Biomaterials* **1995,** 16, (16), 1211-1216.
21. Tanase, C. E.; Spiridon, I. *Materials Science and Engineering: C* **2014,** 40, (0), 242-247.
22. Badami, A. S.; Kreke, M. R.; Thompson, M. S.; Riffle, J. S.; Goldstein, A. S. *Biomaterials* **2006,** 27, (4), 596-606.
23. Heath, D. J.; Christian, P.; Griffin, M. *Biomaterials* **2002,** 23, (6), 1519-1526.
24. Hutmacher, D. W.; Schantz, T.; Zein, I.; Ng, K. W.; Teoh, S. H.; Tan, K. C. *Journal of Biomedical Materials Research* **2001,** 55, (2), 203-216.
25. Duarte, A. R. C.; Mano, J. F.; Reis, R. L. *The Journal of Supercritical Fluids* **2010,** 54, (3), 282-289.
26. Sarasam, A.; Madihally, S. V. *Biomaterials* **2005,** 26, (27), 5500-5508.
27. Ratner, b. D.; Hoffman, A. S.; Schoen, F. J.; Lemons, J. E., *Biomaterial Science*. second edition ed.; 2004.
28. Lee, J. H.; Jung, H. W.; Kang, I.-K.; Lee, H. B. *Biomaterials* **1994,** 15, (9), 705-711.
29. Yuan, Y.; Zhang, P.; Yang, Y.; Wang, X.; Gu, X. *Biomaterials* **2004,** 25, (18), 4273-4278.
30. Storey, R. F.; Sherman, J. W. *Macromolecules* **2002,** 35, (5), 1504-1512.
31. BOUA-IN, K.; CHAIYUT, N.; KSAPABUTR, B. *OPTOELECTRONICS AND ADVANCED MATERIALS – RAPID COMMUNICATIONS* **2010,** 4, (9), 1404 - 1407.

32. Cai, G.; Jiang, H.; Tu, K.; Wang, L.; Zhu, K. *Macromolecular Bioscience* **2009,** 9, (3), 256-261.
33. Wu, Y.; Zheng, Y.; Yang, W.; Wang, C.; Hu, J.; Fu, S. *Carbohydrate Polymers* **2005,** 59, (2), 165-171.